Int. J. Morphol.,
43(6):1909-1919, 2025.

Trifolium pratense L. Extract Improves Propofol-Induced Neuroprotection via Regulating GRP78/ ATF-6 and Bax-bcl2/p53 Signaling in Ischemic Brain Injury in Rats

El Extracto de *Trifolium pratense* L. Mejora la Neuroprotección Inducida por Propofol Mediante la Regulación de la Señalización de GRP78/ATF-6 y Bax-bcl2/p53 en la Lesión Cerebral Isquémica en Ratas

Jiangang Li[1] & Jiaojiao Zhai[1]

LI, J. & ZHAI, J. *Trifolium pratense* L. extract improves propofol-induced neuroprotection via regulating GRP78/ ATF-6 and Bax-bcl2/p53 signaling in ischemic brain injury in rats. *Int. J. Morphol., 43(4)*:1909-1919, 2025.

SUMMARY: This study aimed to investigate the protective effects of *Trifolium pratense* L. extract (TPE) against damage caused by propofol in the hippocampal neurons of rats. A total of fifty Wistar rats were randomly assigned to five groups: a sham group, a TPE-supplemented group receiving 400 mg/kg of TPE, a Propofol-supplemented group receiving 50 mg/kg/h via intravenous injection, an ischemic stroke-reperfusion (IS/R) group modeled after middle cerebral artery occlusion (MCAO), and two MCAO groups treated with 400 mg/kg TPE and 50 mg/kg/h Propofol, with each group consisting of ten rats. Cognitive function was evaluated using the Y-maze test, which assessed the rats' ability to navigate the maze. Rats subjected to IS/R showed a significant delay in completing the maze compared to the normal group. The MCAO group exhibited markedly increased levels of pro-inflammatory cytokines, such as interleukin-1β (IL-1β), IL-6, and tumor necrosis factor-α (TNF-α), alongside decreased levels of anti-inflammatory cytokines (IL-4 and IL-10) and neurotrophic growth factors, including brain-derived neurotrophic factor (BDNF) and glial cell line-derived neurotrophic factor (GDNF). In contrast, the group treated with 400 mg/kg TPE and Propofol after IS/R showed improvements, including elevated levels of neurotrophic growth factors and a favorable alteration in the gene expression profiles of inflammatory and apoptotic markers (such as glucose-regulated protein 78 (GRP78), activating transcription factor 6 (ATF-6), Bcl-2, Bax, and p53) when compared to the IS/R group. These findings suggest that TPE extract may alleviate cognitive deficits following IS/R in rats, potentially through the modulation of inflammatory factors secreted by microglia.

KEY WORDS: Trifolium pretense L; Seeds oil; Inflammation; Apoptosis; Cerebral ischemic stroke -reperfusion.

INTRODUCTION

Ischemic stroke remains one of the leading causes of morbidity and mortality worldwide, posing a significant public health challenge. The World Health Organization (WHO) reports that approximately 15 million people experience a stroke each year, underscoring its critical status, particularly given the high rates of recurrence among survivors (Mendelson & Prabhakaran, 2021; Rabie *et al*., 2025). The mechanisms underlying cerebral ischemic injury are complex and multifaceted, involving inflammatory responses, oxidative stress, excitotoxicity, and mitochondrial dysfunction. During ischemic strokes, the overproduction of reactive oxygen species (ROS) exacerbates oxidative stress, leading to apoptosis and cell death during cerebral ischemia-reperfusion injury (CIS/R) (Orellana-Urzúa *et al*., 2020). Key damaging processes include excitotoxicity and inflammatory responses driven by cytokines such as interleukin-β beta (IL-1β) and tumor necrosis factor-alpha (TNF-α). Cerebral stroke and CIS/R are characterized by intricate mechanisms that include apoptosis, neurotrophic factors, and stress responses (Pawluk *et al*., 2025). The principal apoptotic pathways implicated in neuronal death involve proteins such as Bax, Bcl-2, p53, and caspase-3. Research utilizing rodent models has demonstrated that manipulating these pathways—such as enhancing Bcl-2 levels or inhibiting p53—can significantly mitigate brain injury. Neurotrophic factors, particularly brain-derived neurotrophic factor (BDNF) and glial cell-derived neurotrophic factor (GDNF), play essential roles in neuronal survival and recovery post-stroke, with therapies aimed at increasing their levels showing promising results (Yan *et al*., 2021).

[1] Department of Anesthesiology, Xi'an Fengcheng Hospital, Xi'an City, Shaanxi Province, China.

Received: 2025-07-29 Accepted: 2025-09-04

GRP78 (Glucose-Regulated Protein 78) serves as a chaperone protein that alleviates endoplasmic reticulum (ER) stress by facilitating protein folding and preventing apoptosis. In rodent models of ischemic stroke, increased expression of GRP78 has been observed as a protective response. Elevating GRP78 levels has been associated with reduced neuronal apoptosis and smaller infarct sizes, highlighting its potential as a therapeutic target (Zhang *et al*., 2021). Similarly, ATF-6 (Activating Transcription Factor 6) becomes activated during ER stress, promoting the expression of protective genes such as GRP78. Studies have shown that modulation of the ATF-6 pathway can influence the severity of brain injury, offering a novel strategy for mitigating ER stress-related damage in stroke (Yu *et al*., 2025).

The exploration of traditional herbal medicines has gained momentum, driven by their potential for drug development due to their ability to target multiple pathways, create synergistic effects, and adopt a holistic approach. This multifaceted nature presents advantages over conventional methods that often focus on a single target or compound. *Trifolium pratense* L. extract (TPE), derived from a plant in the *Fabaceae* family, is native to Eastern Europe, Asia, and Northern Africa, thriving in humid to semi-humid environments and producing pinkish-white flowers from July to September. TPE is rich in proteins, vitamins, carbohydrates, and minerals, making it advantageous for food products, antimicrobial films, and high-quality oil production (Akbaribazm *et al*., 2021; Jones *et al*., 2020).

Liquid chromatography-electrospray ionization tandem mass spectrometry (LC-ESI-MS/MS) analysis has identified a variety of bioactive compounds in TPE, including isoflavonoids (such as daidzein and luteolin), flavonoids (like apigenin and quercetin), saponins, carotenoids, essential fatty acids, anthocyanins, and amygdalin derivatives (Akbaribazm *et al*., 2020). Predominantly used in Asia, particularly China, TPE has demonstrated efficacy in treating ischemic heart diseases, providing anti-anginal effects, enhancing antioxidant and anti-inflammatory responses, and improving coronary flow velocity (Situmorang *et al*., 2021). Studies indicate that TPE can prevent acute myocardial infarction in rats by reducing infarct size and inhibiting myocardial cell apoptosis. Its anti-inflammatory and anti-apoptotic properties are attributed to the inhibition of IL-6 and TNF-α, leading to the downregulation of nuclear factor kappa B (NF-κB) and modulation of apoptotic pathways involving mitogen-activated protein kinases (MAPKs) and the phosphoinositide-3-kinase–protein kinase B/Akt (PI3K-PKB/Akt) signaling pathways (Wang *et al*., 2021). This study aims to investigate which bioactive compounds from TPE reach injured brain tissue and contribute to neuroprotection following its administration. Specifically, the research focuses on how TPE enhances Propofol-induced neuroprotection by regulating GRP78/ATF-6 and Bax-Bcl2/p53 signaling pathways in ischemic brain injury in rats.

MATERIAL AND METHOD

Preparation of TPE. Fresh flowers of *Trifolium pratense* L. (3000 grams) were initially dried at 40 °C in a dark environment following authentication by a botanist. The dried flowers were then finely ground using a soil grinder. This powder was combined with a 50:50 ethanol/acetone solution (v/v) and incubated at 38 °C for 48 h. After incubation, the mixture was filtered through a paper filter and concentrated using a rotary evaporator. The resulting extract, weighing 700 g, was stored at 4 °C (Akbaribazm *et al*., 2020).

Middle cerebral artery occlusion (MCAO). The rats were weighed and then anesthetized intraperitoneally using chloral hydrate (400 mg/kg) sourced from Merck, Germany. The middle cerebral artery occlusion (MCAO) procedure was conducted according to the method outlined by Sheikh *et al*. (2019). During the procedure, a 3–0 silicone-coated nylon suture was microscopically inserted through the stump of the external carotid artery. The suture was advanced approximately 20–22 mm into the internal carotid artery past the carotid bifurcation until slight resistance was encountered, indicating that the tip had reached the anterior cerebral artery, effectively obstructing blood flow to the middle cerebral artery. After 60 minutes of ischemia, reperfusion was initiated by carefully retracting the suture. Throughout the surgical procedure, rectal temperature was monitored with a Citizen-513w thermometer and was maintained at 37.0°C using surface heating and cooling methods (Sheikh *et al*., 2019).

Experimental design. Fifty male Wistar rats, each weighing 195 ± 15 g, were randomly assigned to five groups (n=10 per group). Prior to the commencement of the study, the rats underwent a 24-hour acclimatization period to adapt to the study environment, which included temperature, food, and water conditions. They were housed in propylene cages at a temperature of 23 ± 4 °C with a relative humidity of 30 ± 5 %, and maintained on a 12-hour light/dark cycle. The rats had unrestricted access to standard pellets and tap water. All care and euthanasia procedures were carried out with the approval and supervision of the Xi'an Fengcheng Hospital ethics committee, adhering strictly to established protocols for laboratory animal care. Fifty Wistar rats were randomly divided into five groups: a sham, a TPE-supplemented group (receiving 400 mg/kg TPE), a Propofol-supplemented group (receiving 50 mg/kg/h, i.v.), an ischemic stroke-reperfusion (IS/R) group with middle cerebral artery occlusion (MCAO)

model, and two MCAO groups treated with 400 mg/kg TPE and 50 mg/kg/h, i.v. Propofol, each comprising 10 rats (Akbaribazm *et al*., 2020b; Abdelsameea *et al*., 2023).

Morris water maze test. The modified Morris water maze, a widely recognized method for assessing spatial learning and memory (Othman *et al*., 2022), was employed in this study from day 20 to day 40 following ischemic stroke-reperfusion (IS/R). The maze consisted of a circular tank measuring 120 cm in diameter and 50 cm in depth, situated in a quiet, dark room with distinct visual cues. The water temperature was maintained at 23 ± 4 °C. A black, round platform (10 cm in diameter) was submerged 2 cm below the water surface in a fixed location at the center of one quadrant throughout the training phase. The swimming paths of the rats were recorded using a video camera linked to a computer, and the data were analyzed using image processing software. Each rat underwent training sessions twice daily for five consecutive days. In each trial, the rat was placed in the pool facing the wall from one of four randomly selected starting positions and allowed to swim. The time taken to locate the hidden platform, referred to as escape latency, was recorded, with a maximum limit of 90 seconds. If a rat failed to find the platform within this time frame, it was guided to the platform and allowed to stay there for 15 seconds, with its escape latency noted as 90 seconds. One day after the final training session, the platform was removed, and a 90-second probe test was conducted to evaluate memory retention. During this probe trial, the frequency with which the rats crossed the area where the platform had been located was also recorded (Zhang & Dong, 2024; Othman *et al*., 2022).

Glutathione peroxidase (GPx), Catalase (CAT), and Superoxide dismutase (SOD) serum activity. A competitive enzyme immunoassay kit from Mybiosource (Mybiosource Inc., San Diego, California, USA) was utilized to assess the serum activity of glutathione peroxidase (GPx) (Cat no. MBS744364). This kit operates on the interaction between a polyclonal anti-GPX antibody and a GPX-HRP conjugate. To perform the assay, 100 µL of serum samples, standard kit solutions, and PBS (as a blank control) were added to each well. Subsequently, 10 mL of the balance solution provided in the kit was added exclusively to the wells containing the serum samples. Following this, 50 µL of the conjugated solution was introduced to all wells and incubated for 60 min at 37 °C. The absorbance of the final mixture was then measured at 450 nm using an ELISA reader (Biotek Instruments, United States) and reported as U/mL (You *et al*., 2025).

For measuring the serum activity of catalase (CAT), a fluorometric assay kit from Mybiosource (Cat no. MBS2567662; Mybiosource Inc., San Diego, California, USA) was employed. In this procedure, 100 µL of the standard solution (containing 100 µmol/L H_2O_2 in distilled water), 25 µL of serum samples, and 25 µL of chromogen-containing buffer solution were added separately to each well. Additionally, 25 µL of distilled water was added to the wells with the standard solution, while 25 µL of chromogen buffer was added to the wells with serum samples. The contents of the wells were mixed gently and incubated for 5 min at 37 °C. Finally, the absorbance of the mixture was measured at 535 nm using a fluorescence microplate reader (FLUOstar OPTIMA multidetection microplate reader, BMG LABTECH, Germany) and reported as U/mL (Cui *et al*., 2022).

To evaluate the serum activity of superoxide dismutase (SOD), another ELISA kit from Mybiosource (Cat no. MBS705758; Mybiosource Inc., San Diego, California, USA) was utilized. This kit relies on the reaction between a polyclonal anti-SOD antibody and a GPX-HRP conjugate. For this assay, 50 µL of the standard solution and serum samples were added separately to each well, followed by the addition of 50 µL of HRP-conjugate to each well. The contents were mixed gently for 60 s and incubated for 40 min at 37 °C. Afterward, 90 µL of TMB substrate was added to each well and incubated for an additional 20 min at 37 °C. Finally, 50 µL of stop solution was added to the mixture, and after 5 min of incubation at 37 °C, the absorbance of the resulting mixture was measured at 450 nm using a microplate reader (Biotek Instruments, United States) and reported as U/mL (Cui *et al*., 2022).

Serum levels of nitric oxide (NO). In the current study, the Griess colorimetric method was employed to quantify nitric oxide levels. In this procedure, zinc oxide (6 mg of $ZnSO_2$) was added to 500 µL of serum samples, which were then centrifuged at 10,000 ×g for 15 min. The resulting supernatant was mixed with the Griess reagent, consisting of 50 µL of N-(1-naphthyl) ethylenediamine dihydrochloride (5 mM), 50 µL of sulfanilamide (20 mM), and 100 µL of vanadium chloride (40 mM), and incubated for 60 min at 37 °C. Finally, the absorbance of the mixture was measured at 540 and 630 nm using a spectrophotometer (Shimadzu UV-1800, Shimadzu, Japan) and reported as µM/mL (Cui *et al*., 2022).

Liver tissue thiol, lipid peroxidation levels [thiobarbituric acid reactive substances (TBARS)], and total antioxidant capacity (FRAP levels) levels. The measurement of thiobarbituric acid reactive substances (TBARS) was employed to assess the level of lipid peroxidation. In this procedure, the liver and kidneys were homogenized using a tissue homogenizer, and 100 µL of the resulting homogenate was mixed with a TBARS solution consisting of 50 µL of

phosphoric acid, 50 µL of 0.02 mol/L thiobarbituric acid, and 2 µL of 0.19 mol/L butylated hydroxytoluene. The mixture was then incubated at 37 °C for 30 min and subsequently centrifuged at 12,000 rpm for 10 min. The absorbance of the final solution was measured at 532 nm using a spectrophotometer (Shimazu, UV-1800, Shimadzu, Japan) and expressed in nmol/mg (You *et al*., 2025).

The FRAP method was utilized to determine the total antioxidant capacity (TAC). Following the procedure outlined in section 2.7, 200 µL of homogenized liver and kidney tissue was added to the FRAP solution. This mixture was incubated for 15 min at 25°C and then centrifuged at 10,000 rpm for 15 min. The absorbance of the final solution was recorded at 593 nm with a spectrophotometer (Shimazu, UV-1800, Shimadzu, Japan) and reported as µmol/mg of protein.

To measure thiol levels, which serve as an important antioxidant marker, 100 µL of homogenized brain tissue was combined with 20 µL of 5,5'-dithiobis-(2-nitrobenzoic acid) (DTNB). The mixture was incubated at 37 °C for 15 min and then centrifuged at 12,000 g for 5 min. The absorbance of the supernatant was assessed at 412 nm using an ELISA reader (You *et al*., 2025).

Serum concentrations of GDNF, BDNF, TNF-α, IL-4, IL-1β, IL-10, and IL-6. Serum was obtained by centrifuging blood samples at 10,000 g for 20 min. The levels of glial cell-derived neurotrophic factor (GDNF) (Cat. No.: ab244211) and brain-derived neurotrophic factor (BDNF) (Cat. No.: ab108319) in the serum were quantified using ELISA kits from Abcam (Abcam, USA). The assays were performed following the manufacturer's guidelines and protocols. To assess the anti-inflammatory effects of VASO, we measured the levels of various cytokines using rodent-specific sandwich ELISA kits from Novus Biologicals (USA). Specifically, we quantified the anti-inflammatory cytokines interleukin-10 (IL-10) (Cat. No.: R1000) and interleukin-4 (IL-4) (Cat. No.: NBP1-91171), as well as the pro-inflammatory cytokines interleukin-1 beta (IL-1β) (Cat. No.: RLB00), tumor necrosis factor-alpha (TNF-α) (Cat. No.: NBP2-DY410), and interleukin-6 (IL-6) (Cat. No.: M6000B), in accordance with the protocol provided (Sun *et al*., 2019).

Glucose-regulated protein 78 (GRP78), activating transcription factor 6 (ATF-6), Bcl-2, Bax, and p53. Total RNA was extracted using Trizol, following the manufacturer's instructions (Ambion, China). Five micrograms of the isolated RNA were converted into cDNA using random primers. Quantitative real-time PCR was conducted with SYBR Green (Vazyme, China) on an ABI7900 fluorescence PCR system (CA, USA). The PCR cycling conditions were as follows: an initial 2 min at 50 °C, followed by 10 min at 95 °C, and then 40 cycles consisting of 30 s at 95 °C and 30 sat 60 °C. Gene expression levels were normalized to GAPDH. The primer sequences utilized were:

ATF-6: Forward: ATGAGCGGATCCGCGAGAC; Reverse: TCAGGAGCAGCTGTTGTCCT
P53: Forward: GGAAGACAGGCCCAGACTAT; Reverse: GCTCGACGCTAGGATCTGAC
Bax: Forward: GCCGAGGATGATTGCTGAC; Reverse: TCTCCAGCCATGATGGGTT
Bcl-2: Forward: AGGAGGAGTGTGAGGAGGAG; Reverse: TGGAGGAGGAGGAGGAGAG
GRP78: Forward: ATGAGTCCACACCCAGAA; Reverse: TCACTGCGGATAGCAGAG
GAPDH: Forward: TGAAGGTCGGAGTCAACGG; Reverse: AGAGTTAAAAGCAGCCCTGGTG

Relative gene expression levels were calculated using the threshold cycle (Ct) method, along with the DDCt and fold change formulas.

The fold formula change = $2^{-\Delta\Delta CT}$; $\Delta\Delta Ct$ = [(Ct sample - Ct GAPDH gene) - (Ct sample – Ct control)] (Zhang & Dong, 2024).

Immunohistochemical examination. To assess oxidative stress-induced apoptosis in liver and kidney tissues, immunohistochemical staining was conducted for p53-positive cells. The procedure involved fixing the tissues in 10 % formalin for 72 h, followed by standard tissue processing. Paraffin-embedded sections of liver and kidney tissues were sliced into 5 µm-thick sections and subjected to an antigen retrieval process at 95 °C for 24 h. To inhibit endogenous peroxidases, all slides were treated with 3 % H_2O_2 for 3 min. Subsequently, the slides were incubated with a rodent-specific monoclonal antibody against p53 (dilution 1:200, Santa Cruz Biotechnology) for 45 min at room temperature. After this, the slides were treated with 5 % bovine serum albumin for 5 min to block any unbound antibodies, followed by incubation in chromogen (3, 3'-diaminobenzidine) for 30 minutes at 37 °C. Counterstaining was performed using hematoxylin, and 50 random fields of view were evaluated using a light microscope (Olympus CH3, Japan) equipped with a camera (Moticam Technologies, Japan). The proportion of p53-positive cells was calculated as (p53 positive cells/total cells) × 100 at a magnification of 400 ×, and results were reported as means (%) ± SEM.

Brain histopathology. In this study, methylene blue and Golgi's staining was employed to analyze brain tissue, emphasizing neuronal structures and cellular details. Initially, brain tissues were fixed in 10 % paraformaldehyde for a

duration of 24 to 48 h, followed by washing with phosphate-buffered saline (PBS). The tissues were then dehydrated using a graded series of ethanol solutions and subsequently cleared with xylene or an alternative clearing agent. The samples were embedded in paraffin and sectioned into slices of 5 - 10 µm thickness using a microtome (LEICA SM2010RV1.2, Germany), after which they were rehydrated. In methylene blue staining, the sections were stained with a 1% methylene blue solution for 10 to 20 minutes, rinsed in PBS, re-dehydrated, cleared, and mounted using a mounting medium and coverslip. In Golgi's brain tissue staining method, brain tissue sections are immersed in a solution of potassium dichromate and silver nitrate, typically for 24 to 48 h, allowing the silver chromate to precipitate within the neurons. Following this incubation, the sections are rinsed in distilled water, dehydrated through a series of alcohol solutions, cleared in xylene, and then embedded in paraffin. Once embedded, the tissue is cut into thin sections, which are then mounted on glass slides. Histological analysis was performed using a light microscope at magnifications of ¥100 and ¥400. Images were captured with an Olympus CH3 calibrated light microscopy system (Olympus, Japan) and processed using Moticam software (Moticam Technologies, Japan) (El-Shetry *et al*., 2021).

Statistical analysis. Data analysis was conducted using SPSS software version 16 (SPSS, IBM, Chicago, USA), while GraphPad Prism version 8 was utilized for graph creation. The normality of the data was assessed using the Kolmogorov-Smirnov test. Subsequently, one-way analysis of variance (ANOVA) was performed to evaluate changes in mean differences across all groups, followed by Tukey's *post-hoc* analysis. A p-value of less than 0.05 was considered statistically significant, and the results were presented as mean ± standard error of the mean (SEM).

RESULTS

Synergistic effects of TPE and Propofol in MCAO - induced spatial cognitive deficits. To assess the effects of MCAO and TPE treatment on cognitive performance, we conducted the Morris water maze test after a 50-day treatment period. Throughout the daily training sessions, all rats exhibited a gradual reduction in escape latency, with significant differences noted among the groups. One-way ANOVA analysis indicated that from day 4 onward, the normal group demonstrated a markedly shorter latency in finding the platform compared to the MCAO group ($p < 0.05$), with similar results on day 5 ($p < 0.05$), suggesting memory impairment associated with MCAO. On days 4 and 5, the escape latency in the MCAO + TPE + Propofol group was significantly longer ($p < 0.05$), while the MCAO + TPE and MCAO + Propofol groups did not show significant differences compared to the MCAO group ($p > 0.05$). This implies that the MCAO + TPE + Propofol treatment effectively enhanced spatial learning throughout the 5-day training period (Fig. 1a). Furthermore, in the probe test where the platform was removed, rats in the MCAO group crossed the area where the platform had been less frequently than those in the normal group ($p < 0.05$). Conversely, rats treated with MCAO + TPE + Propofol crossed the platform location more often than those in the MCAO group ($p < 0.05$), indicating an improvement in spatial memory (Fig. 1b).

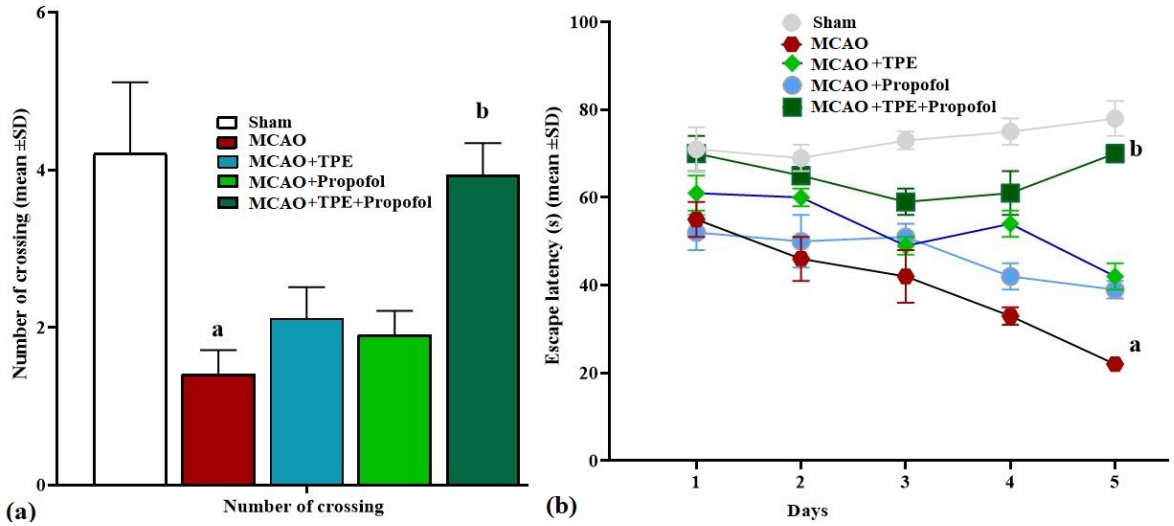

Fig. 1. (a) The number of crossing and (b) Escape latency (s) (means ± SD; n=10/group) in experimental groups. [a]($p<0.05$) MCAO *vs.* sham groups; [b]($p<0.05$) TPE and Propofol treated *vs*. MCAO groups.

Synergistic effects of TPE and Propofol on serum concentrations of GDNF and BDNF. MCAO was found to inhibit the secretion of neurotrophic factors in the brain by activating apoptotic pathways in glial cells, resulting in a significant decrease ($p < 0.05$) in serum levels of GDNF and BDNF compared to the sham group. In contrast, treatment with TPE, in synergy with Propofol, led to an increase in serum concentrations of GDNF and BDNF, underscoring TPE's strong capacity to stimulate and protect glial cells. Importantly, the MCAO + TPE + Propofol group exhibited a significant increase ($p < 0.05$) in GDNF and BDNF levels compared to the MCAO group (Fig. 2a).

Synergistic effects of TPE and Propofol on serum concentrations of TNF-α, IL-6, IL-10, and IL-1β. MCAO induced inflammatory responses, resulting in elevated levels of pro-inflammatory cytokines while simultaneously inhibiting the activity of systemic anti-inflammatory cytokines. This led to a significant increase ($p < 0.05$) in serum concentrations of TNF-α, IL-1β, and IL-6 when compared to the sham group, along with a notable decrease ($p < 0.05$) in IL-10 and IL-4 levels. In the MCAO + TPE group, TPE treatment reduced serum levels of TNF-α and IL-6 compared to the MCAO group, although this reduction was not statistically significant ($p > 0.05$), indicating MCAO's potent anti-inflammatory effects. Furthermore, TPE treatment progressively enhanced the levels of IL-10 and IL-4 while decreasing pro-inflammatory cytokines (IL-1β, TNF-α, and IL-6). These effects were significantly pronounced ($p < 0.05$) when TPE was combined with Propofol in the MCAO + TPE + Propofol group compared to the MCAO group (Fig. 2b).

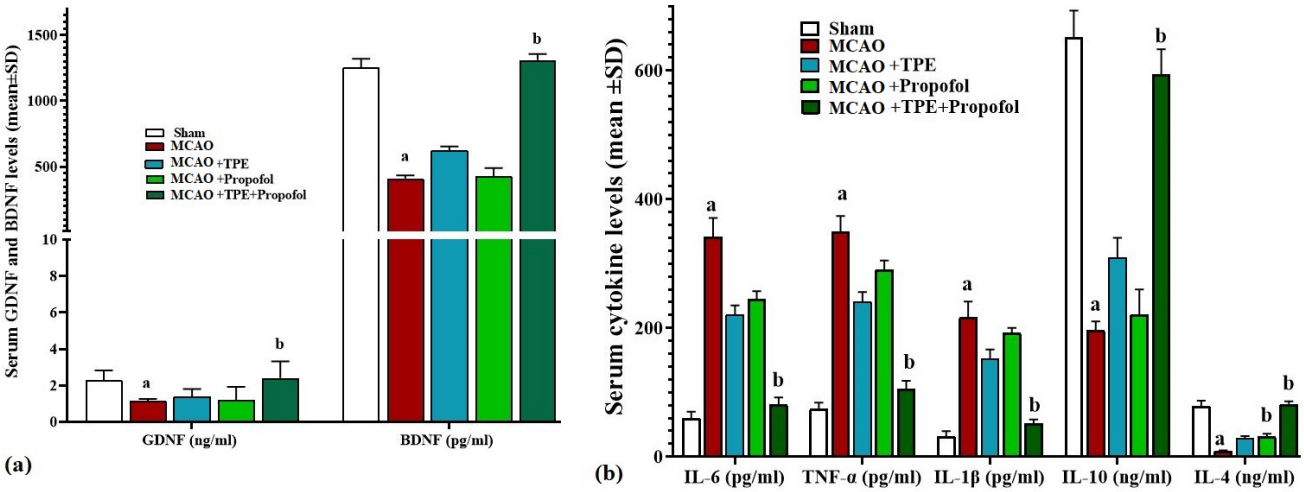

Fig. 2. (a) Serum levels of GDNF (ng/ml) and BDNF (pg/ml) and (b) Serum levels of IL-1β, TNF-β, IL-6 (pg/ml), IL-10, and IL-4 (ng/ml) (means ± SD; n=10/group) in experimental groups. [a]($p<0.05$) MCAO *vs*. sham groups; [b]($p<0.05$) TPE and Propofol treated *vs*. MCAO groups.

Synergistic effects of TPE and Propofol on serum GPx, CAT, and SOD activity alongside serum NO levels. MCAO stimulated the generation of free radicals, leading to a notable increase in serum nitric oxide (NO) levels compared to the sham group. In contrast, treatment with TPE and Propofol (in the MCAO + TPE + Propofol group) resulted in a reduction of NO concentrations relative to the MCAO group. Both TPE alone and its combination with Propofol significantly lowered ($p < 0.05$) serum NO levels, highlighting TPE's strong antioxidant capabilities. Furthermore, MCAO significantly diminished the serum activity of all three antioxidant enzymes when compared to the sham rats. However, treatment with TPE and Propofol increased the serum levels of these enzymes, with a significant rise ($p < 0.05$) observed in the MCAO + TPE + Propofol group compared to the MCAO group (Fig. 3a).

Synergistic effects of TPE and Propofol on brain thiol, FRAP, and TBARS levels.
Levels of thiol, FRAP, and TBARS were assessed as crucial indicators of overall antioxidant capacity and lipid peroxidation (LPO). The findings indicated that MCAO significantly ($p < 0.05$) lowered the levels of these markers in tissues compared to the sham group. In contrast, due to their strong antioxidant effects, both TPE and Propofol, whether used alone or in combination, resulted in increased levels of these markers when compared to the MCAO group. This increase was significant ($p < 0.05$) in the MCAO + TPE + Propofol group (Fig. 3b).

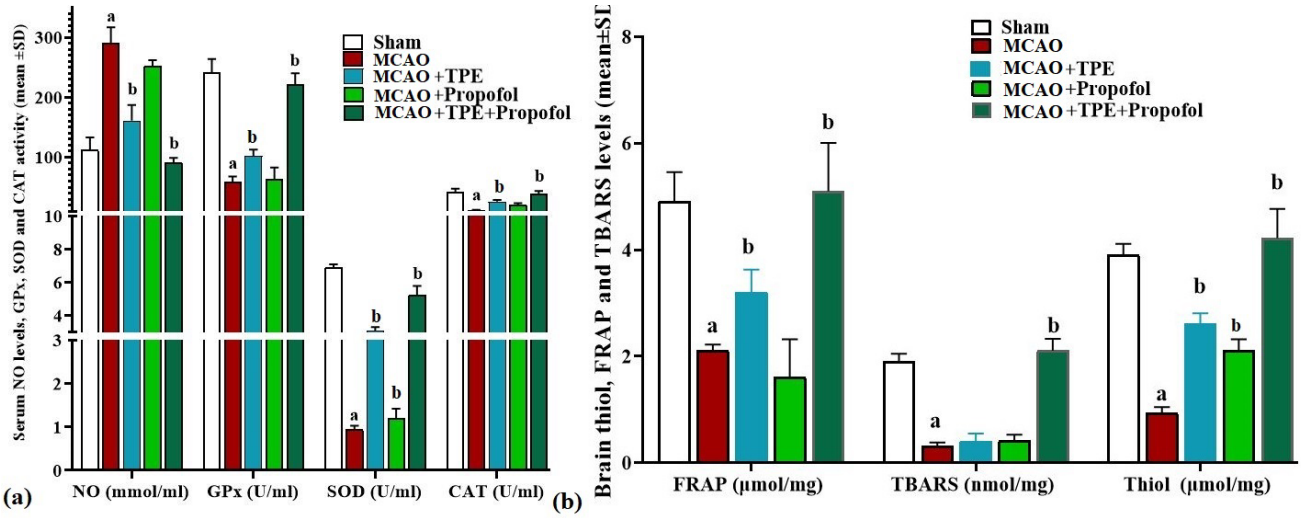

Fig. 3. (a) Serum levels of NO (mmol/ml), alongside the mean serum activity of SOD, CAT, and GPx (U/ml) and (b) Brain tissue levels of TBARS (nmol/mg), thiol (µmol/mg) and FRAP (µmol/mg) (means ± SD; n=10/group) in experimental groups. a ($p<0.05$) MCAO *vs.* sham groups; b ($p<0.05$) TPE and Propofol treated *vs.* MCAO groups.

Synergistic effects of TPE and Propofol on expression of brain Bcl-2, Bax, IL-6, GRP78, ATF-6, and p53 genes

Gene expression analysis targeting apoptosis, oxidative stress, and metabolic pathways in glial and neural cells demonstrated that MCAO treatment resulted in a significant increase in the expression of Bax, ATF-6, GRP78, and p53, while Bcl-2 levels were significantly decreased in the brain compared to the sham group ($p < 0.05$). The most pronounced changes were noted in the MCAO + TPE + Propofol group, where the expressions of Bax, ATF-6, GRP78, and p53 were significantly elevated ($p < 0.05$), whereas Bcl-2 expression was significantly reduced ($p < 0.05$) compared to the MCAO group (Fig. 4).

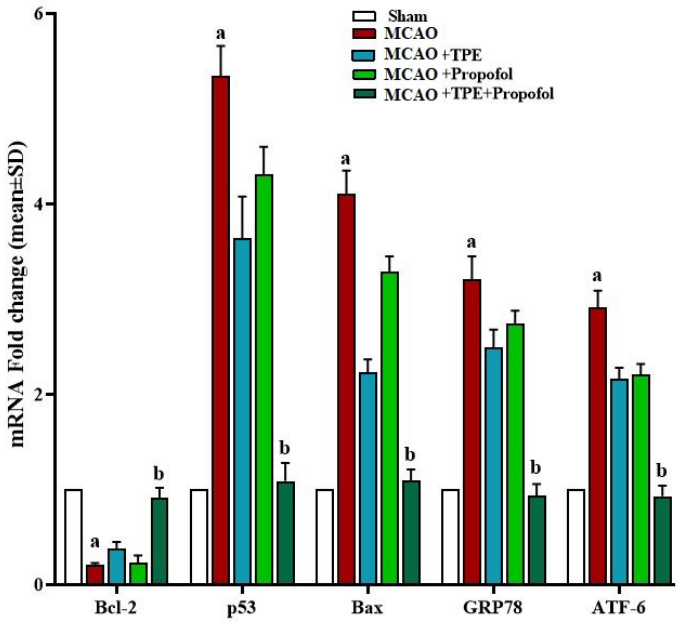

Fig. 4. Bax, Bcl-2, ATF-6, GRP78, and p53 genes expression in brain (means ± SD; n=10/group) in experimental groups. [a]($p<0.05$) MCAO *vs*. sham groups; [b]($p<0.05$) TPE and Propofol treated *vs.* MCAO groups.

Synergistic effects of TPE and Propofol on expression of brain p53 expression. Following the assessment of apoptotic indices through IHC staining, it was observed that the MCAO group exhibited a significant increase in the percentage of p53-positive cells compared to the sham group ($p < 0.05$). In contrast, TPE treatment in both the MCAO + TPE and MCAO + TPE + Propofol groups significantly decreased ($p < 0.05$) the percentage of p53 immunopositive cells relative to the MCAO group, highlighting its protective effects (Fig. 5).

Brain histopathological evaluations. Histopathological analysis of brain tissue revealed that MCAO treatment resulted in lymphocytic infiltration (LI), vascular damage, neurons exhibiting pyknotic nuclei and vacuolated cytoplasm, apoptotic bodies (AP), and degenerated neurons near necrotic areas (N). The MCAO group displayed significant neuronal atrophy and a marked reduction in the density of normal parenchyma compared to the sham group. Conversely, co-treatment with TPE and Propofol enhanced neuronal parenchyma density and reduced the occurrence of apoptotic bodies, neuronal degeneration, and LI compared to the MCAO group (Fig. 6).

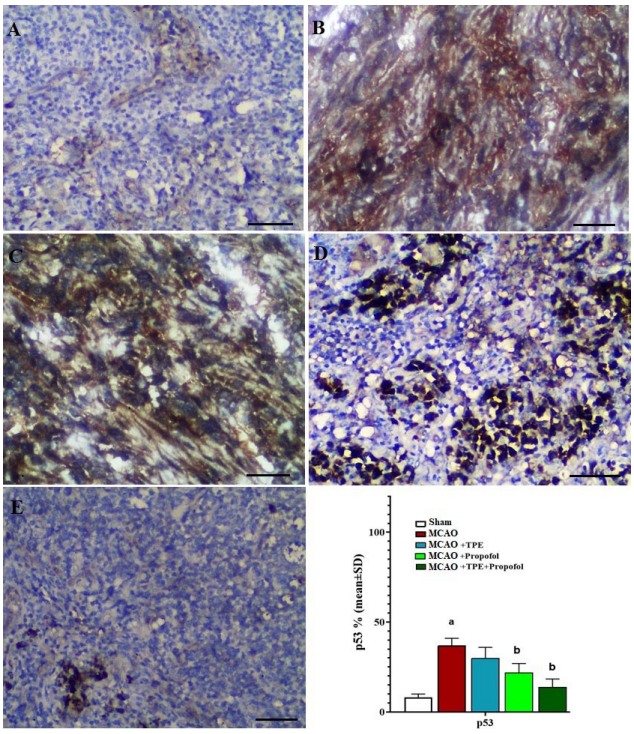

Fig. 5. Impact of TPE and Propofol in p53 positive cells in brain in sham (A), MCAO (B), MCAO + TPE (C), MCAO + Propofol (D), MCAO + TPE + Propofol (E) (Scale bar = 50 µm, DAB staining ¥ 400). [a]($p<0.05$) MCAO vs. sham groups; [b]($p<0.05$) TPE and Propofol treated *vs*. MCAO groups.

DISCUSSION

Our research highlights the effectiveness of TPE in preserving normal neuronal function in the brain by enhancing antioxidant, anti-inflammatory and anti-apoptotic pathways. This indicates a strong neuroprotective role of TPE against damage induced by MCAO, affecting both brain physiology and structure.

In this investigation, administering 400 mg/kg of TPE alongside Propofol significantly improved behavioral performance, particularly noted at 20 and 40 days' post-treatment. Furthermore, notable enhancements in micro-anatomy were observed at the 400 mg/kg dosage. To our knowledge, this is the first report demonstrating TPE's capacity to maintain neuron density following MCAO, especially at this dosage. MCAO, commonly resulting from strokes, disrupts neuronal impulse transmission by obstructing blood flow to certain brain areas, leading to degeneration of nerve cells in those regions. Studies have indicated that inflammation and oxidative stress can hinder neuronal plasticity in the hippocampus, contributing to infarct expansion (Yang *et al*., 2022a). TPE is acknowledged for its anti-inflammatory, anti-apoptotic, and antioxidant properties, as supported by various studies. Additionally, TPE has been shown to inhibit gliosis and prevent the destruction of neuronal nuclei in arsenic neurotoxicity models (Al-Shami *et al*., 2023). The anti-inflammatory effects of TPE are primarily attributed to flavonoids, while its antioxidant benefits are linked to both flavonoid and phenolic compounds. Tian *et al*. (2022), demonstrated in an in vitro study that TPE functions as an anti-cholinesterase and anti-apoptotic prodrug, showcasing neuroprotective effects and enhancing the survival of PC12 neurons (Tian *et al*., 2022). de Rus Jacquet *et al*. (2021), found that TPE boosts the antioxidant capacity of glial cells and neurons by increasing the activity of cytochrome C oxidase, superoxide dismutase (SOD), and succinate dehydrogenase. This enhancement in antioxidant activity protects these cells from oxidative damage and free radical injury associated with

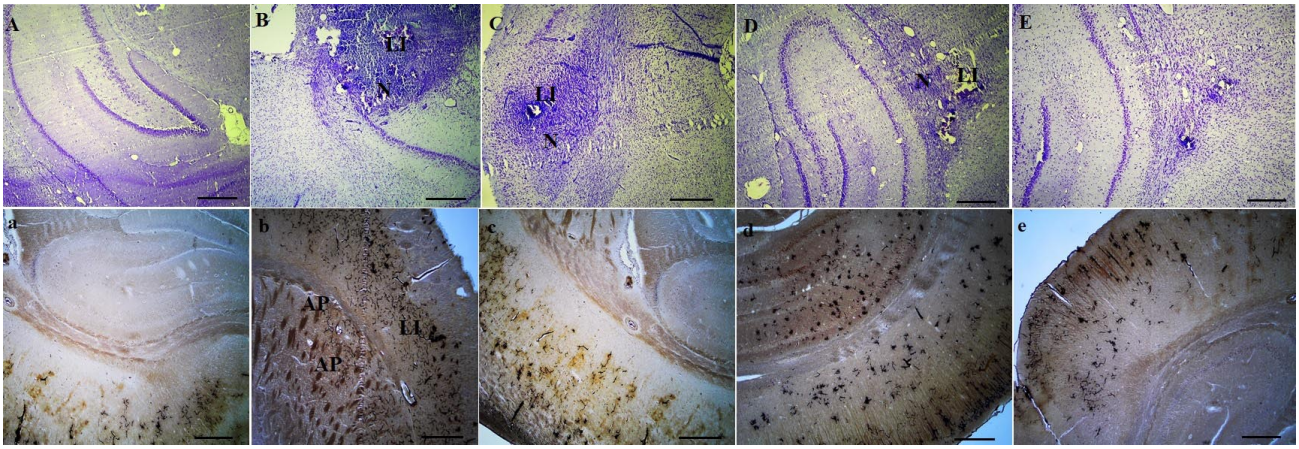

Fig. 6. Histopathological changes in brain tissue in sham (A, a), MCAO (B, b), MCAO + TPE (C, c), MCAO + Propofol (D, d), and MCAO + TPE + Propofol (E, e) groups [upper raw: methylene blue staining × 100 (with scale bar = 200 µm); lower raw: Golgi's staining × 100 (with scale bar = 200 µm)]. Apoptotic bodies (AP), lymphatic infiltration (LI), and degenerated neurons adjacent to necrotic areas (N).

permanent occlusion of cerebral arteries (de Rus Jacquet *et al*., 2021). In research by Yang *et al*. (2022b), utilizing the MCAO model, extracts from Vaccinium myrtillus were shown to elevate malondialdehyde levels and Na+-K+-ATPase activity in brain tissue, enhancing antioxidant capacity, exhibiting anti-apoptotic effects, and reducing cleaved caspase-3 gene expression (Yang *et al*., 2022b). Our findings suggest that pre-treatment with TPE before a MCAO event can mitigate apoptosis and enhance performance in behavioral assessments. Genistein, a primary flavonoid in TPE, has been found to increase GPx levels and reduce lipid peroxidation by inhibiting the NF-kB pathway in rat brains (Jiang *et al*., 2021). Additionally, biochanin A, quercetin, and apigenin have been shown to elevate norepinephrine and serotonin levels by modulating oxidative stress in an Alzheimer's model (Dourado *et al*., 2020). In our study, we induced MCAO and evaluated the resulting neurobehavioral changes in rats through various behavioral metrics.

The MCAO procedure significantly impaired animal behavior, reflected in deficits in functional status, neurological impairments, locomotor performance, and exploratory behavior as assessed by the Morris water maze test. However, pretreatment with TPE at a dosage of 400 mg/kg combined with Propofol nearly restored these experimental parameters to baseline levels. Animal studies have indicated that TPE inhibits caspase-9 and cytochrome c, thereby reducing mitochondrial apoptosis and preventing neurodegeneration of hippocampal neurons (Zhou *et al*., 2021). This study also emphasized TPE's role in enhancing cognitive function related to the striatum and hippocampus due to its neuroprotective properties. In a separate investigation, Khazaei *et al*. (2022), examined TPE's protective effects against diabetes-induced testis damage in BALB/c mice. They reported that 400 mg/kg doses of TPE significantly increased total antioxidant capacity, boosted the activity of endogenous antioxidant enzymes, and reduced apoptosis, as evidenced by decreased p53 expression in testicular tubular cells (Khazaei *et al*., 2022). Similarly, Akbaribazm *et al*. (2020), found that TPE at 400 mg/kg effectively diminished lipid peroxidation in breast cancer cells in mice caused by doxorubicin, thereby inhibiting mitochondrial apoptosis through suppression of the Bex-Bcl-2/p53/caspase-3 pathway in 4T1 lineage (Akbaribazm *et al*., 2020). In our current study, TPE was observed to elevate endogenous antioxidant enzyme levels by enhancing antioxidant capacity, leading to a reduction in p53 and Bax gene expression in hippocampal cells. These protective effects of TPE suggest its potential as an anti-infarct agent. Previous research has indicated that the observed behavioral recovery and reduction in infarct volume may be associated with TPE's ability to preserve dopaminergic receptors and maintain neurotransmitter levels (Mardi *et al*., 2023). However, our study did not assess neurotransmitter levels, and further investigation is necessary to fully elucidate the mechanisms of IS/R in limiting infarct areas. TPE, administered at 400 mg/kg with Propofol, also stimulated the secretion of GDNF and BDNF. MCAO is known to elevate free radical production, resulting in oxidative stress and subsequent membrane lipid peroxidation, which compromises membrane integrity and function. Our results demonstrate that TPE exhibits neuroprotective properties by maintaining neuron density in the hippocampus. Newairy *et al*. (2020), illustrated that TPE reduces carbonyl content and lipid peroxidation while enhancing levels of antioxidant enzymes, such as superoxide dismutase, catalase, and glutathione, collectively improving the survival of rat brain neurons (Newairy *et al*., 2020). The increase in neuronal density in the hippocampus following TPE treatment is likely due to TPE's inactivation of inflammatory mediators. The interaction between IS/R and hippocampal regions in the affected groups further suggests that TPE enhanceshippocampal neuronal activity by preserving synaptic plasticity among neurons, facilitating the replacement of damaged areas. In this study, TPE at a dosage of 400 mg/kg was also found to bolster the metabolic/antioxidant pathway dependent on GRP78 and ATF-6, which protects brain neuron function and structure against ischemic damage caused by IS/R. Consequently, TPE improved animal movement performance and reduced infarct sizes by promoting neuronal recovery in the hippocampus. As previously mentioned, the active components of TPE, including quercetin, genistein, and apigenin glycosides, are believed to contribute to its neuroprotective effects. These effects correlate with tissue concentrations of FRAP and TBARS levels, as well as serum levels of GPx, CAT, and SOD, further validating the efficacy of TPE treatment.

CONCLUSION

The findings of this study demonstrate that TPE significantly enhances the neuroprotective effects of propofol in the context of ischemic brain injury in rats. The administration of TPE not only improved cognitive function, as evidenced by performance in the Morris water maze test, but also positively influenced the expression of neurotrophic factors and modulated inflammatory and apoptotic pathways. Specifically, TPE was shown to regulate key signaling molecules such as GRP78, ATF-6, Bax, Bcl-2, and p53, contributing to a reduction in neuronal apoptosis and inflammation. These results suggest that TPE may serve as a promising adjunct therapy in the management of ischemic stroke, potentially improving outcomes through its multifaceted protective mechanisms. Further research is warranted to elucidate the precise bioactive compounds involved and their specific roles in neuroprotection, paving the way for novel therapeutic strategies in stroke management.

ETHICAL APPROVAL. The experimental protocols of this study were approved by the Xi'an Fengcheng Hospital ethics committee.

LI, J. & ZHAI, J. El extracto de *Trifolium pratense* L. mejora la neuroprotección inducida por propofol mediante la regulación de la señalización de GRP78/ATF-6 y Bax-bcl2/p53 en la lesión cerebral isquémica en ratas. *Int. J. Morphol., 43(6)*:1909-1919, 2025.

RESUMEN: Este estudio tuvo como objetivo investigar los efectos protectores del extracto de *Trifolium pratense* L. (TPE) contra el daño causado por Propofol en las neuronas del hipocampo de ratas. Un total de cincuenta ratas Wistar fueron asignadas aleatoriamente a cinco grupos: un grupo simulado, un grupo suplementado con TPE que recibió 400 mg/kg de TPE, un grupo suplementado con Propofol que recibió 50 mg/kg/h por vía intravenosa, un grupo de ictus isquémico-reperfusión (IS/R) modelado a partir de la oclusión de la arteria cerebral media (MCAO), y dos grupos MCAO tratados con 400 mg/kg de TPE y 50 mg/kg/h de Propofol, con cada grupo compuesto por diez ratas. La función cognitiva se evaluó mediante la prueba del laberinto en Y, que evaluó la capacidad de las ratas para navegar por el laberinto. Las ratas sometidas a IS/R mostraron un retraso significativo en completar el laberinto en comparación con el grupo normal. El grupo MCAO mostró niveles notablemente elevados de citoquinas proinflamatorias, como la interleucina-1β (IL-1β), la IL-6 y el factor de necrosis tumoral-α (TNF-α), junto con una disminución de los niveles de citoquinas antiinflamatorias (IL-4 e IL-10) y factores de crecimiento neurotrófico, incluyendo el factor neurotrófico derivado del cerebro (BDNF) y el factor neurotrófico derivado de la línea celular glial (GDNF). Por el contrario, el grupo tratado con 400 mg/kg de TPE y Propofol tras IS/R mostró mejoras, incluyendo niveles elevados de factores de crecimiento neurotrófico y una alteración favorable en los perfiles de expresión génica de marcadores inflamatorios y apoptóticos (como la proteína regulada por glucosa 78 (GRP78), el factor de transcripción activador 6 (ATF-6), Bcl-2, Bax y p53) en comparación con el grupo IS/R. Estos hallazgos sugieren que el extracto de TPE podría aliviar los déficits cognitivos tras el ictus isquémico cerebral/reperfusión en ratas, posiblemente mediante la modulación de factores inflamatorios secretados por la microglia.

PALABRAS CLAVE: *Trifolium pretense* L; Aceite de semillas; Inflamación; Apoptosis; Ictus isquémico cerebral-reperfusión.

REFERENCES

Abdelsameea, A. A.; Alsemeh, A. E.; Desouky, M.; Samy, W.; Fawzy, A. & Abbas, N. A. Paeonol preconditioning alleviates partial hepatic ischemia/reperfusion injury in rats: The role of inhibition of autophagy and TLR4/MyD88/NF-kB pathway. *Zagazig Univ. Med. J., 29(4)*:983-93, 2023.

Akbaribazm, M.; Khazaei, M. R. & Khazaei, M. *Trifolium pratense* L. (red clover) extract and doxorubicin synergistically inhibit proliferation of 4T1 breast cancer in tumor-bearing BALB/c mice through modulation of apoptosis and increase antioxidant and anti-inflammatory related pathways. *Food Sci. Nutr., 8(8)*:4276-90, 2020.

Akbaribazm, M.; Khazaei, F.; Naseri, L.; Pazhouhi, M.; Zamanian, M. & Khazaei, M. Pharmacological and therapeutic properties of the red clover (*Trifolium pratense* L.): An overview of the new findings. *J. Tradit. Chin. Med., 41(4)*:642-9, 2021.

Cui, D.; Xu, Z.; Qiu, S. & Sun, Y. Nasturtium officinale L. and metformin alleviate the estradiol-induced polycystic ovary syndrome with synergistic effects through modulation of Bax/Bcl-2/p53/caspase-3 signaling pathway and anti-inflammatory and anti-oxidative effects. *J. Food Biochem., 46(12)*:e14462, 2022.

de Rus Jacquet, A.; Ambaw, A.; Tambe, M. A.; Ma, S. Y.; Timmers, M.; Grace, M. H.; Wu, Q. L.; Simon, J. E.; McCabe, G. P.; Lila, M. A.; Shi, R. & Rochet, J. C. Neuroprotective mechanisms of red clover and soy isoflavones in Parkinson's disease models. *Food Funct., 12(23)*:11987-2007, 2021.

Dourado, N. S.; Souza, C. D. S.; de Almeida, M. M. A.; Bispo da Silva, A.; Dos Santos, B. L.; Silva, V. D. A.; De Assis, A. M.; da Silva, J. S.; Souza, D. O.; Costa, M. F. D.; Butt, A. M. & Costa, S. L. Neuroimmunomodulatory and neuroprotective effects of the flavonoid apigenin in in vitro models of neuroinflammation associated with Alzheimer's disease. *Front. Aging Neurosci., 12*:119, 2020.

El-Shetry, E. S.; Mohamed, A. A.; Khater, S. I.; Metwally, M. M. M.; Nassan, M. A.; Shalaby, S.; A M El-Mandrawy, S.; Bin Emran, T. & M Abdel-Ghany, H. Synergistically enhanced apoptotic and oxidative DNA damaging pathways in the rat brain with lead and/or aluminum metals toxicity: Expression pattern of genes OGG1 and P53. *J. Trace Elem. Med. Biol., 68*:126860, 2021.

Jiang, T.; Xu, S.; Shen, Y.; Xu, Y. & Li, Y. Genistein attenuates isoflurane-induced neuroinflammation by inhibiting TLR4-mediated microglial polarization in vivo and *in vitro*. *J. Inflamm. Res., 14*:2587-600, 2021.

Jones, C.; De Vega, J.; Lloyd, D.; Hegarty, M.; Ayling, S.; Powell, W.; & Skøt, L. Population structure and genetic diversity in red clover (*Trifolium pratense* L.) germplasm. Sci. Rep., 10(1):8364, 2020.

Rabie, S. B.; Kang, HC.; Choi, M.; & Suk, H. Assessing the efficacy of pharmacist-engaged interventions in influencing antibiotic prescribing behavior among general practitioners: meta-analysis. *Int. J. Clin. Med., 3(3)*:52-65, 2025.

Khazaei, M. R.; Gravandi, E.; Ghanbari, E.; Niromand, E. & Khazaei, M. *Trifolium pratense* extract increases testosterone and improves sperm characteristics and antioxidant status in diabetic rats. Biotechnic Histochem., 97(8), 576-83. *Biotech Histochem., 97(8)*:576-83, 2022.

Mardi, S.; Salemi, Z. & Palizvan, M. R. Antioxidant properties of Trifolium resupinatum and its therapeutic potential for Alzheimer's disease. *Folia Neuropathol., 61(1)*:37-46., 2023.

Mendelson, S. J. & Prabhakaran, S. Diagnosis and management of transient ischemic attack and acute ischemic stroke: A review. *JAMA, 325(11)*:1088-98, 2021.

Newairy, A. S. A.; Hamaad, F. A.; Wahby, M. M. & Abdou, H. M. The potential therapeutic effect of red clover's extract against an induced molecular neurodegeneration in male rats. *Swed. J. Biosci. Res., 1(1)*:39-50., 2020.

Orellana-Urzúa, S.; Rojas, I.; Líbano, L. & Rodrigo, R. Pathophysiology of ischemic stroke: Role of oxidative stress. *Curr. Pharm. Des., 26(34)*:4246-60, 2020.

Othman, M. Z.; Hassan, Z.; Has, A. T. C. Morris water maze: A versatile and pertinent tool for assessing spatial learning and memory. *Exp. Anim., 71(3)*:264-80, 2022.

Pawluk, H.; Wozniak, A.; Tafelska-Kaczmarek, A.; Kosinska, A.; Pawluk, M.; Sergot, K.; Grochowalska, R. & Koodziejska, R. The role of IL-6 in ischemic stroke. *Biomolecules, 15(4)*:470, 2025.

Sheikh, A. M.; Yano, S.; Mitaki, S.; Haque, M. A.; Yamaguchi, S. & Nagai, A. A mesenchymal stem cell line (B10) increases angiogenesis in a rat MCAO model. *Exp. Neurol., 311*:182-93, 2019.

Situmorang, H.; Hestiantoro, A.; Purbadi, S.; Flamandita, D. & Sahlan, M. In-silico dynamic analysis of Sulawesi propolis as anti-endometriosis drug: Interaction study with TNF alpha receptor, NF-kB, estrogen receptor, progesterone receptor, and prostaglandin receptor. *Ann. Med. Surg., 67*:102459, 2021.

Sun, R. T.; Piao, X. Y.; Cai, M.; Li, Y. & Luo, S. W. Effects of Salvia miltiorrhiza on cerebral infarction volume, nerve behavior, and SOD, GSH-px, MDA, BDNF, and GDNF in rats. J. *Hainan Med. Univ., 25(14)*:15-8, 2019.

Tian, J.; Wang, X. Q. & Tian, Z. Focusing on formononetin: Recent perspectives for its neuroprotective potentials. *Front. Pharmacol., 13*:905898, 2022.

Wang, X.; Li, T. & Dong, K. Effect of formononetin from *Trifolium pratense* L. on oxidative stress, energy metabolism, and inflammatory response after cerebral ischemia-reperfusion injury in mice. *Food Sci. Technol., 42*:e57821, 2021.

Yang, L.; Li, M.; Zhan, Y.; Feng, X.; Lu, Y.; Li, M.; Zhuang, Y.; Lei, J. & Zhao, H. The impact of ischemic stroke on gray and white matter injury correlated with motor and cognitive impairments in permanent MCAO rats: A multimodal MRI-based study. *Front. Neurol., 13*:834329, 2022a.

Yang, S. E.; Lien, J. C.; Tsai, C. W. & Wu, C. R. Therapeutic potential and mechanisms of novel simple O-substituted isoflavones against cerebral ischemia reperfusion. *Int. J. Mol. Sci., 23(18)*:10394, 2022b.

Yu, X.; Dang, L.; Dhar, A.; Zhang, R.; Xu, F.; Spasojevic, I.; Sheng, H. & Yang, W. Activation of ATF6 signaling confers long-term beneficial effects in young and aged mice after permanent stroke. *Transl. Stroke Res., 16(5)*:1799-810, 2025.

Zhang, J. & Dong, B. Effects of Vaccinium arctostaphylos L. seeds oil on cerebral stroke in rats: A biochemical, immunohistochemical, and molecular approach. *Int. J. Morphol., 42(6)*:1773-82, 2024.

Zhang, Y. M.; Xu, H.; Chen, S. H. & Sun, H. Electroacupuncture regulates endoplasmic reticulum stress and ameliorates neuronal injury in rats with acute ischemic stroke. *Evid. Based Complement. Alternat. Med., 2021*:9912325, 2021.

Zhou, Y.; Xu, B.; Yu, H.; Zhao, W.; Song, X.; Liu, Y.; Wang, K.; Peacher, N.; Zhao, X. & Zhang, H. T. Biochanin A attenuates ovariectomy-induced cognition deficit via antioxidant effects in female rats. *Front. Pharmacol., 12*:603316., 2021.

Corresponding author:
Dr. Jiaojiao Zhai
Department of Anesthesiology
Xi'an Fengcheng Hospital
Xi'an City
Shaanxi Province 710016
CHINA
E-mail: zhaijiao0110@outlook.com

ORCID ID: 0009-0001-2081-6395